

Original Article



# Treatment with 3-Bromo-4,5-Dihydroxybenzaldehyde Improves Cardiac Function by Inhibiting Macrophage Infiltration in Mice

Ningning Ji , BSc, Honghong Lou , BSc, Xinyan Gong , BSc, Ting Fu , MS, and Shimao Ni , PhD

Department of Cardiology, Yiwu Hospital of Wenzhou Medical University (Yiwu Central Hospital), Yiwu, China

OPEN ACCESS

**Received:** Dec 10, 2017  
**Revised:** Mar 28, 2018  
**Accepted:** Apr 10, 2018

**Correspondence to**  
Shimao Ni, PhD

Department of Cardiology, Yiwu Hospital of Wenzhou Medical University (Yiwu Central Hospital), 699, Jiangdong Road, Yiwu 322000, China.

E-mail: 1793870950@qq.com

Copyright © 2018. The Korean Society of Cardiology

This is an Open Access article distributed under the terms of the Creative Commons Attribution Non-Commercial License (<https://creativecommons.org/licenses/by-nc/4.0>) which permits unrestricted noncommercial use, distribution, and reproduction in any medium, provided the original work is properly cited.

**ORCID iDs**

Ningning Ji   
<https://orcid.org/0000-0002-2412-1582>  
Honghong Lou   
<https://orcid.org/0000-0002-6891-8120>  
Xinyan Gong   
<https://orcid.org/0000-0003-2311-4265>  
Ting Fu   
<https://orcid.org/0000-0002-2242-4387>  
Shimao Ni   
<https://orcid.org/0000-0003-2274-7183>

**Conflict of Interest**

The authors have no financial conflicts of interest.

## ABSTRACT

**Background and Objectives:** Appropriate inflammatory response is necessary for cardiac repairing after acute myocardial infarction (MI). Three-Bromo-4,5-dihydroxybenzaldehyde (BDB) is a potent antioxidant and natural bromophenol compound derived from red algae. Although BDB has been shown to have an anti-inflammatory effect, it remains unclear whether BDB affects cardiac remodeling after MI. The aim of this study was to investigate the potential role of BDB on cardiac function recovery after MI in mice.

**Methods:** Mice were intraperitoneally injected with BDB (100 mg/kg) or vehicle control respectively 1 hour before MI and then treated every other day. Cardiac function was monitored by transthoracic echocardiography at day 7 after MI. The survival of mice was observed for 2 weeks and hematoxylin and eosin (H&E) staining was used to determine the infarct size. Macrophages infiltration was examined by immunofluorescence staining. Enzyme-linked immunosorbent assay (ELISA) was used to test the production of cytokines associated with macrophages. The phosphorylation status of nuclear factor (NF)- $\kappa$ B was determined by western blot.

**Results:** BDB administration dramatically improved cardiac function recovery, and decreased mortality and infarcted size after MI. Treatment with BDB reduced CD68<sup>+</sup> macrophages, M1 and M2 macrophages infiltration post-MI, and suppressed the secretion of pro-inflammatory cytokines, such as tumor necrosis factor (TNF)- $\alpha$ , interleukin (IL)-1 $\beta$ , monocyte chemoattractant protein (MCP)-1, and IL-6 in the injured hearts. Furthermore, BDB inhibited the phosphorylation of NF- $\kappa$ B in the infarcted hearts.

**Conclusions:** These data demonstrate, for the first time, that BDB treatment facilitated cardiac healing by suppressing pro-inflammatory cytokine secretion, and indicate that BDB may serve as a therapeutic agent for acute MI.

**Keywords:** Myocardial infarction; 3-Bromo-4,5-Dihydroxybenzaldehyde; Macrophages

## INTRODUCTION

Myocardial infarction (MI) is one of the leading causes of death in the world. Acute MI leads to an acute inflammatory response, which is very important for heart debris clearance, repair and regeneration.<sup>1)</sup> As early as 30 minutes after coronary artery ligation, neutrophils

**Author Contributions**

Data curation: Ji N, Lou H, Fu T, Ni S; Formal analysis: Ji N; Resources: Gong X, Ni S; Software: Ni S; Writing - original draft: Ji N, Ni S.

are recruited to the infarcted myocardium and macrophages shortly thereafter in response to chemokines and cytokines produced by apoptotic cardiomyocytes. The number of neutrophils peak 24 hours after MI, whereas that of macrophages peak around 3 days after MI and then drops to the normal count after 2 weeks. In addition, activated macrophages release abundant pro-inflammatory cytokines such as tumor necrosis factor (TNF)- $\alpha$ , monocyte chemoattractant protein (MCP)-1, interleukin (IL)-1 $\beta$ , and IL-6, which participate in phagocytosis and the clearance of necrotic debris.<sup>2)</sup> Following the acute inflammatory response, the infarcted myocardium is subjected to structural self-remodeling processes including collagen deposition, angiogenesis, and scar formation.<sup>3)</sup> Thus, macrophages serve as a central cellular protagonist for cardiac repair after ischemia and maybe a potential therapeutic target for acute MI.

3-Bromo-4,5-dihydroxybenzaldehyde (BDB) is a simple natural compound derived from red algae (e.g. *Rhodomela confervoides*, *Polysiphonia morrowii*, and *Polysiphonia urceolata*)<sup>4-6)</sup> and supposed to be a potent antioxidant in human keratinocytes.<sup>7)</sup> BDB has attracted increasing interest for its pharmacological effects including amelioration of redox-mediated damage to cells or tissues, suppression of apoptosis, and antimicrobial activity against the hematopoietic necrosis virus.<sup>6)8)9)</sup> Recently, BDB was reported to ameliorate 2,4-dinitrochlorobenzene-induced atopic dermatitis inflammatory responses, reduce the infiltration of macrophages and suppresses the production of IL-6.<sup>10)</sup> However, the role of BDB in acute MI, as well as its effect on macrophages infiltration has not been uncovered.

Therefore, the present study aimed to investigate the effect of BDB on macrophage infiltration and related cytokines production in a mouse model of acute MI.

## METHODS

### Mouse model of MI

A total of 60 adult C57BL/6 genetic background male mice (aged 7–8 weeks) were purchased from Shanghai Laboratory Animal Center (Shanghai, China) and randomized to construct the MI model. All the mice were subjected to permanent left anterior descending artery (LAD) ligation or sham surgery as described previously.<sup>11)</sup> Briefly, the mice were anesthetized with 1.5% isoflurane gas using an induced chamber before being mechanically ventilated with a rodent respirator. Subsequently, the chest cavity was opened to expose the heart and a 6–0 silk suture was used for permanent ligation of the LAD. The suture was passed approximately 2 mm below the tip of the left auricle. Complete vessel occlusion was confirmed by the presence of myocardial blanching in the perfusion bed. The thorax was closed with a 5–0 silk suture. Mice that died within 24 hours after surgery were excluded from the experiment. Sham-operated animals underwent the same procedure without LAD. All the animals were maintained and handled in accordance with the guidelines of the Institutional Animal Care and Use Committee of the Wenzhou Medical University (approval number: 200016-0003).

### BDB administration

BDB was purchased from Matrix Scientific (catalog number: 056469; Colombia, SC, USA). One hundred mg/kg BDB (dissolved in phosphate-buffered saline [PBS]) were administered via intraperitoneal (i.p.) injection 1 hour before MI surgery and then was administrated every other day. By comparison, the control group received the same dose of vehicle.

### Transthoracic echocardiography

Cardiac function was evaluated using a Vevo2100 Ultrasound system (Fujifilm VisualSonics, Bothell, WA, USA) at 7 days after the surgery. The investigator was blinded to group assignment, and each group includes 6–14 mice. Mice were anesthetized by isoflurane inhalation. Two-dimensional parasternal long axis views of the left ventricle (LV) were obtained. The LV internal diameters at end diastole and systole, as well as the interventricular septal wall and posterior wall thicknesses were measured by M-mode tracing.

### Hematoxylin and eosin (H&E) staining

Two weeks after MI, 8–14 mice per group were anesthetized with 5% isoflurane (Merck, Darmstadt, Germany) and 95% oxygen in a gas chamber. The hearts of MI mice were harvested and fixed for 24 hours in 4% paraformaldehyde at 4°C, and then embedded in paraffin. Paraffin-embedded hearts were cut into 6- $\mu$ m-thick sections and detected infarcted sizes by H&E staining. Photomicrographs were obtained using an Olympus microscope (Tokyo, Japan), and the areas were measured by the Image J software (National Institutes of Health, Bethesda, MA, USA). The infarct size was calculated as a percentage of the LV area.

### Terminal deoxynucleotidyl transferase (TdT)-mediated dUTP nick end labeling (TUNEL) staining

For the TUNEL assay, MI heart from mice that were administered vehicle or BDB were embedded in optimal cutting temperature (OCT) compound and frozen, and cut into 6- $\mu$ m-thick sections. The heart sections were stained by using a TUNEL fluorescence In Situ Apoptosis Detection kit (Yeasen, Shanghai, China), according to the manufacturer's instructions.

### Immunofluorescence staining

Heart were harvested at indicated times and were embedded in OCT reagent, and each group includes 8–10 mice. OCT-embedded hearts were cut into 6- $\mu$ m-thick frozen sections using the freezing microtome (Leica Biosystems, Wetzlar, Germany). Frozen sections were fixed 10 minutes in cold acetone, washed with PBS, and incubated in PBS containing 3% bovine serum albumin (BSA) for 40–60 minutes at room temperature to prevent non-specific binding of antibodies. Tissue slides were then incubated with the following primary antibodies: anti-CD68 (1:200; AbDSerotec, Kidlington, UK) antibody at 4°C overnight. The slides were then washed with PBS three times before incubation with Alexa Fluor-conjugated secondary antibodies (1:1,000; Invitrogen, Carlsbad, CA, USA) for 2 hours at room temperature. ProLong Gold antifade reagent with 4',6-diamidino-2-phenylindole (DAPI; Invitrogen) was applied to counterstain the slides. The slides were then mounted and the stained sections were visualized under a laser scanning confocal microscope (Carl Zeiss, Oberkochen, Germany) and analyzed using Image-Pro Plus software (version 6.0; Media Cybernetics, Rockville, MD, USA). At least 3 different heart sections were obtained from each mouse and 6 random images of at the risk areas were taken from each section.

### Flow cytometric analysis

Flow cytometric experiment was performed as previously described (Temporal dynamics of cardiac immune cell accumulation following acute MI). Eight to 10 infarcted hearts each group were cut into pieces and digested at 37°C for 1.5 hours in PBS, containing type II collagenase (1.5 mg/mL; Worthington Biochemical Corporation, Lakewood, NJ, USA), elastase (0.25 mg/mL; Worthington Biochemical Corporation), and DNase I (0.5 mg/mL; Worthington Biochemical Corporation). After digestion, the tissues were passed through a 70  $\mu$ m cell strainer, and leukocyte-enriched fractions were isolated with 37–70% Percoll®

(GE Healthcare Biosciences, Piscataway, NJ, USA) by density gradient centrifugation. Next, the cells were collected from the interface and washed with RPMI-1640 cell culture medium. Isolated cells were then incubated with the following antibodies: CD45-PE (BD Biosciences, San Diego, CA, USA), CD11b-FITC (Miltenyi Biotec, Bergisch Gladbach, Germany), F4/80-BV421 (BioLegend, San Diego, CA, USA), Ly-6G-APC (BD Biosciences), and CD206-PE-cy7 (BD Biosciences) at 4°C for 30 minutes. Flow cytometric analysis and sorting were performed using a FACSAria™ flow cytometer (BD Biosciences), and the data obtained were analysed with FlowJo 7.6.1 software (Tree Star Inc., Ashland, OR, USA).

### Western blot analysis

We grinded the heart tissues (50 mg per heart) from animals in 1 mL of ice-cold homogenization buffer (containing protease inhibitor, calcineurin inhibitors, and phenylmethylsulfonyl fluoride [PMSF]). Homogenates were then centrifuged at 4°C, 9,000 ×g for 30 minutes. Supernatants were collected and centrifuged at 4°C, 14,000 ×g for 30 minutes, and the bicinchoninic acid (BCA) method was used to quantify proteins. Then the same amount protein was mixing with loading buffer and boiled for 10 minutes. We performed sodium dodecyl sulfate polyacrylamide gel electrophoresis (SDS-PAGE) with the sampling amount per well of 50 µg of protein. Then we transferred the proteins to a nitrocellulose (NC) membrane and washed them with Tris-buffered saline and Tween 20 (TBST, 20 mmol/L Tris-HCl [pH7.5], 0.05% Tween 20, and 0.6% NaCl), which consists of 5% skimmed milk powder, at room temperature, and sealed the membrane for 1–2 hours. The membranes were incubated with primary antibody, anti-nuclear factor (NF)-κB (catalog number: #8242, 1:1,000; Cell Signaling Technologies, Danvers, MA, USA), anti-p-NF-κB p65 (catalog number: #3033, 1:1,000; Cell Signaling Technologies), or anti-glyceraldehyde 3-phosphate dehydrogenase (GAPDH, catalog number: #5174, 1:1,000; Cell Signaling Technologies) at 4°C overnight. The membranes were washed 3 times in TBST. The samples were then incubated for 2 hours at room temperature with a horseradish peroxidase (HRP)-conjugated secondary antibody. Blots were visualized by an enhanced chemiluminescence detection system (GE Healthcare Biosciences). The results were analyzed by the professional software Image J to quantify gray value.

### Enzyme-linked immunosorbent assay (ELISA)

The levels of TNF-α, IL-1β, MCP-1, and IL-6 in heart were measured with an ELISA kit following the manufacturer's instructions (R&D Systems, Minneapolis, MN, USA). Briefly, each heart tissue was homogenized by PBS in a 1:10 concentration (0.1 g of tissue to 1 mL of PBS buffer). A monoclonal antibody specific for these proteins was pre-coated into wells. The standards and test samples were then pipetted into the wells to allow binding of these proteins to the immobilized antibodies. After washing away any unbound substances, an enzyme-linked polyclonal antibody specific for these proteins was added to the wells. Following removal of unbound antibody-enzyme reagent by washing 5 times, a substrate solution was added to the wells and color was developed. The optical density of each well was measured at the wave length of 450 or 510 nm on a microreader (S190; Molecular Devices, San Jose, CA, USA). The concentration of each cytokine or chemokine was accordingly calculated.

### Statistical analysis

Data have been expressed as mean±standard error of measurement (SEM). Two-tailed Student's t-test was used for comparisons between different groups. Data were analyzed using GraphPad Prism 5.0 software (GraphPad Software, Inc., San Diego, CA, USA). The p values less than 0.05 were considered as being statistically significant.

## RESULTS

### Treatment with BDB accelerated cardiac recovery after MI

To fully evaluate the effect of BDB on cardiac healing post-MI, BDB (100 mg/kg) or vehicle control was injected into the mice before 1 hour of the LAD ligation and then was administered every other day (Figure 1A). Cardiac function was markedly improved at days 7 after MI in the mice that received BDB than that in the vehicle group. We found that left ventricular ejection fraction (LVEF, 20.51±1.975% vs. 28.84±2.521%;  $p < 0.05$ ) and left ventricular fractional

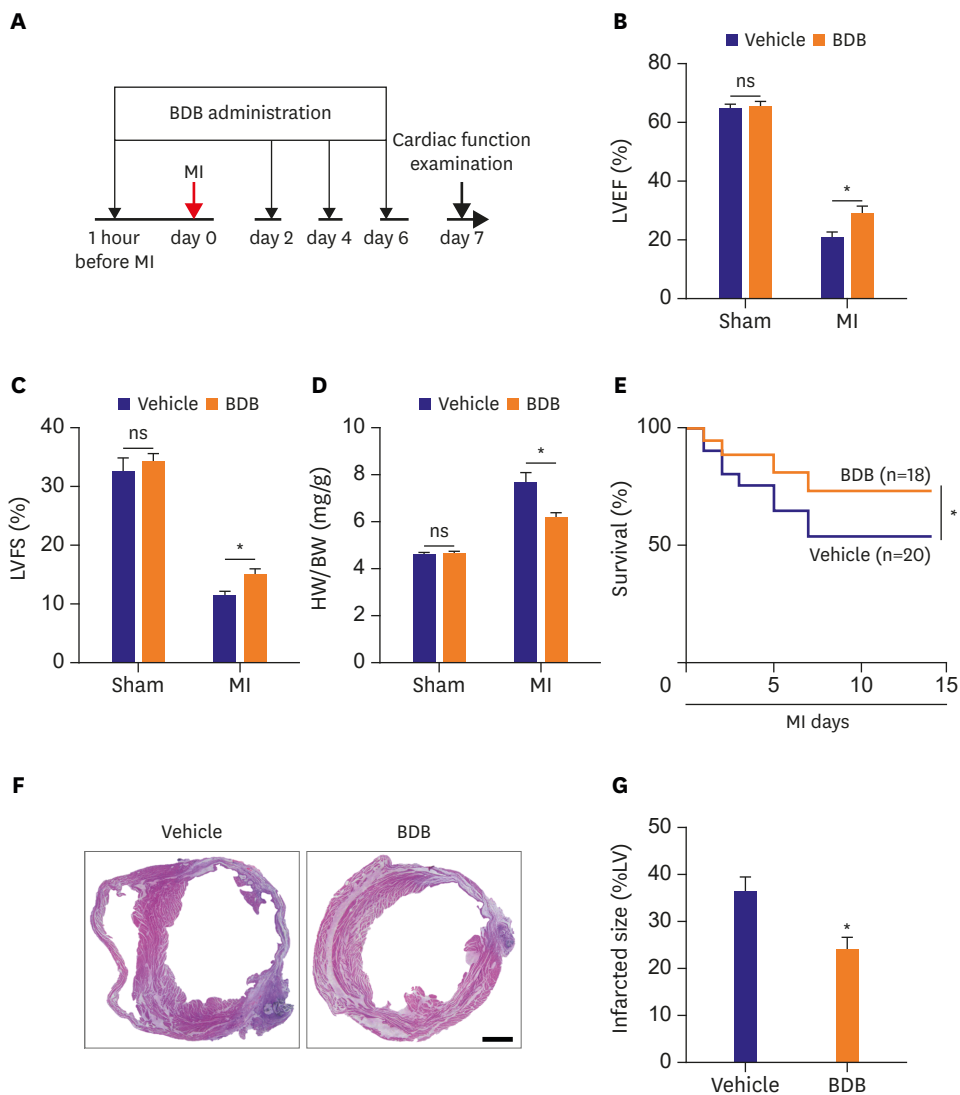


**Figure 1.** BDB treatment improved cardiac recovery after MI in mice. (A) Schematic of protocol for adoptive transfer and administration of BDB to mice. Acute MI was induced by surgical ligation of LAD in mice. (B, C) Cardiac function of vehicle/BDB treatment mice on day 14 after MI. (D) Ratio of HW/BW of mice was measured 14 days after MI. (E) Survival rates after MI in BDB- or vehicle-treated mice. Survival curves up to 2 weeks after MI were created by Kaplan-Meier method and compared by a log-rank test. (F) Representative H&E staining of heart sections from vehicle or BDB treated-mice at 2 weeks after MI (scale bar=1,000  $\mu$ m). (G) Quantitative analysis of infarct size in vehicle and BDB treated-mice at 2 weeks after MI. Data are expressed as mean $\pm$ SEM (n=6-14). BDB = 3-Bromo-4,5-dihydroxybenzaldehyde; H&E = hematoxylin and eosin; HW/BW = heart weight to body weight; LAD = left anterior descending artery; LV = left ventricle; LVEF = left ventricular ejection fraction; LVFS = left ventricular fractional shortening; MI = myocardial infarction; SEM = standard error of measurement. \*The  $p < 0.05$  compared with vehicle group.

shortening (LVFS,  $11.33 \pm 0.765\%$  vs.  $14.96 \pm 1.012\%$ ;  $p < 0.05$ ) after MI significantly improved in the BDB treatment group compared to vehicle treatment (**Figure 1B and C**). A compensatory myocardial hypertrophy always occurs post-MI, which can be assessed by an index of heart weight to body weight (HW/BW) ratio.<sup>12)</sup> The HW/BW ratio after treatment with BDB before MI was much lower than that in the mice treated with vehicle ( $6.1 \pm 0.246\%$  vs.  $7.6 \pm 0.442\%$ ;  $p < 0.05$ ; **Figure 1D**). There was no significant difference between the 2 sham groups.

The survival rate was found to be significantly lower in Vehicle group than in BDB-treated group at 2 weeks (**Figure 1E**). We also observed that the infarct size after MI is significantly decreased in BDB-treated MI group than in vehicle MI group ( $36.15 \pm 3.002\%$  vs.  $23.84 \pm 2.662\%$ ;  $p < 0.05$ ; **Figure 1F and G**). These findings suggest that treatment with BDB exerts a protective effect against heart failure.

In response to MI, different stress response responses are induced and it is important of the cardiomyocytes apoptosis in the damaged heart. To test whether BDB treatment may affect cardiomyocytes apoptosis after acute MI, we performed TUNEL staining in the infarcted heart. However, the percentage of TUNEL-positive cardiomyocytes was not significantly altered in response to the BDB treatment from days 3 post-MI observed (**Figure 2A and B**), suggesting that BDB administration did not affect cardiomyocytes apoptosis after acute MI.

### Treatment with BDB reduced the recruitment of macrophages in the heart of MI

The infiltration of macrophages plays an important role in early cardiac repair after ischemia,<sup>13)</sup> and BDB as an anti-inflammatory agent effective to inhibit allergic diseases in experimental models.<sup>10)</sup> So we detected the infiltration of macrophages in the infarcted hearts after 3 and 7 days post-MI. As expected, the macrophages (CD68<sup>+</sup>) at 3 days after MI were strongly reduced in number at ischemic border zone (BZ) in the infarcted hearts (**Figure 3A and B**). Similarly, the infiltration of macrophages in the infarcted hearts was also blunted by BDB administration 7 days post-MI (**Figure 3C and D**), indicating that the acute inflammatory response to ischemia was suppressed by BDB administration.

It is very important of macrophage polarization in acute MI and distinct macrophage lineages contribute to disparate patterns of cardiac recovery and remodeling in the neonatal and

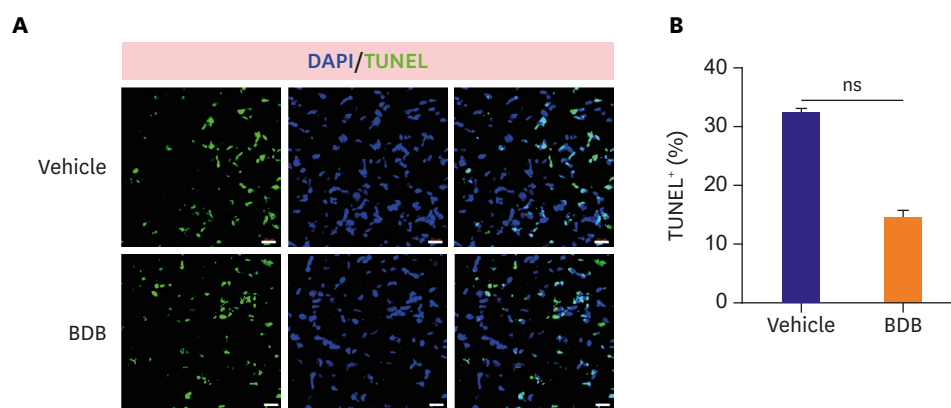


**Figure 2.** BDB treatment did not affect cardiomyocytes apoptosis after MI. (A) Representative TUNEL staining of heart sections from vehicle- and BDB-treated mice at day 3 post-MI (scale bar, 20  $\mu$ m). (B) Quantification of TUNEL<sup>+</sup> cardiomyocytes from (A) (n=6-8).

BDB = 3-Bromo-4,5-dihydroxybenzaldehyde; DAPI = 4',6-diamidino-2-phenylindole; MI = myocardial infarction; ns = not significant; TUNEL = terminal deoxynucleotidyl transferase (TdT)-mediated dUTP nick end labeling.

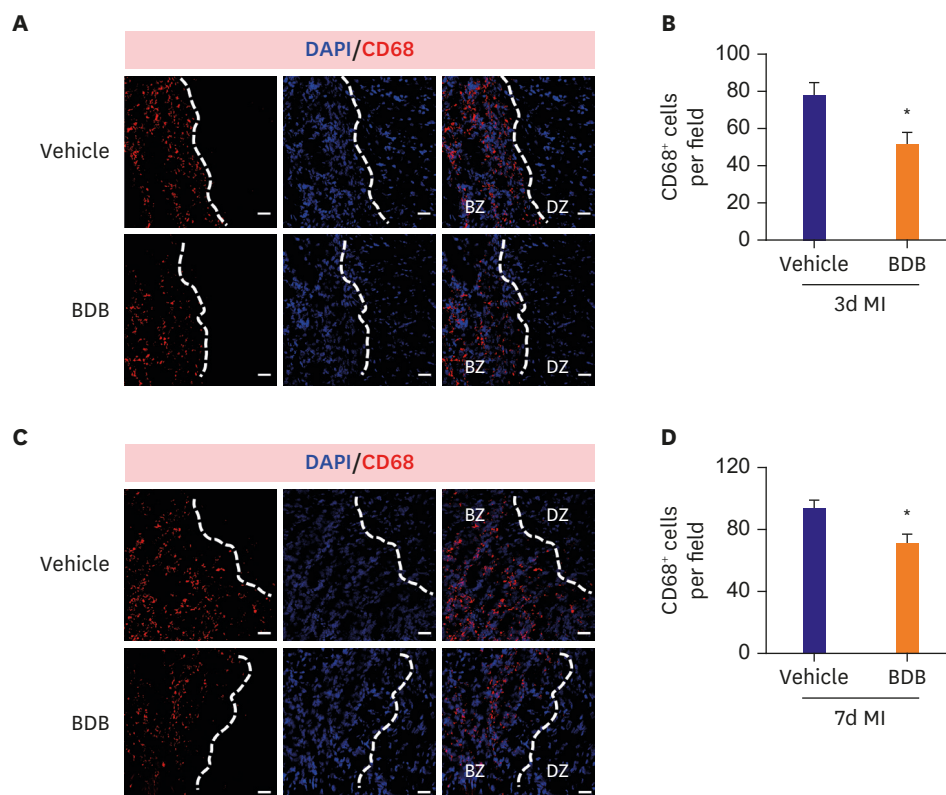


**Figure 3.** BDB treatment reduced macrophages infiltration after MI in mice. The representative CD68 (red) staining images of the infarcted hearts from BDB- or vehicle-treated mice at day 3 (A) and day 7 (C) post-MI (scale bar, 50  $\mu$ m). (B) Quantitation of CD68<sup>+</sup> cells in injured hearts as shown in (A). (D) Quantitation of CD68<sup>+</sup> cells of infarcted hearts as shown in (C). Data are expressed as mean $\pm$ SEM (n=8–10). BDB = 3-Bromo-4,5-dihydroxybenzaldehyde; BZ = ischemic border zone; DAPI = 4',6-diamidino-2-phenylindole; DZ = non-ischemic distant zone; MI = myocardial infarction; SEM = standard error of measurement. \*The p<0.05 compared with vehicle group.

adult heart.<sup>14)</sup> Therefore, we examined the influence of BDB on M1 and M2 macrophage recruitment in hearts after acute MI (Figure 4A). The total number of infiltrating macrophage was markedly suppressed by BDB treatment (Figure 4B). Indeed, both M1 (Figure 4C) and M2 (Figure 4D) recruited into hearts were suppressed in the BDB treatment group during the acute phase after MI (days 3 and 7). These results indicate that BDB facilitated cardiac repair by suppressing the acute inflammatory responses after MI, including the infiltration of M1 and M2 macrophages.

### BDB treatment suppressed the secretion of pro-inflammatory cytokines in the heart post-MI

Macrophages play important roles in the progress of acute MI through secreting a number of cytokines and chemokines.<sup>15)</sup> We examined the levels of TNF- $\alpha$ , IL-1 $\beta$ , MCP-1, and IL-6 at the areas at-risk of the heart tissues. The expression levels of the 4 pro-inflammatory cytokines were significantly decreased in the BDB treatment group compared to vehicle treatment at day 3 and 7 after MI (Figure 5). These results indicated that BDB inhibited the acute inflammatory responses after MI mainly by reducing pro-inflammatory cytokines secretion.

### BDB reduced the phosphorylation of NF- $\kappa$ B in the hearts of MI

To further explore the function of macrophages, we detected the phosphorylation of NF- $\kappa$ B, a protein complex that is important for the generation of pro-inflammatory cytokines,

BDB Improves Cardiac Recovery after MI

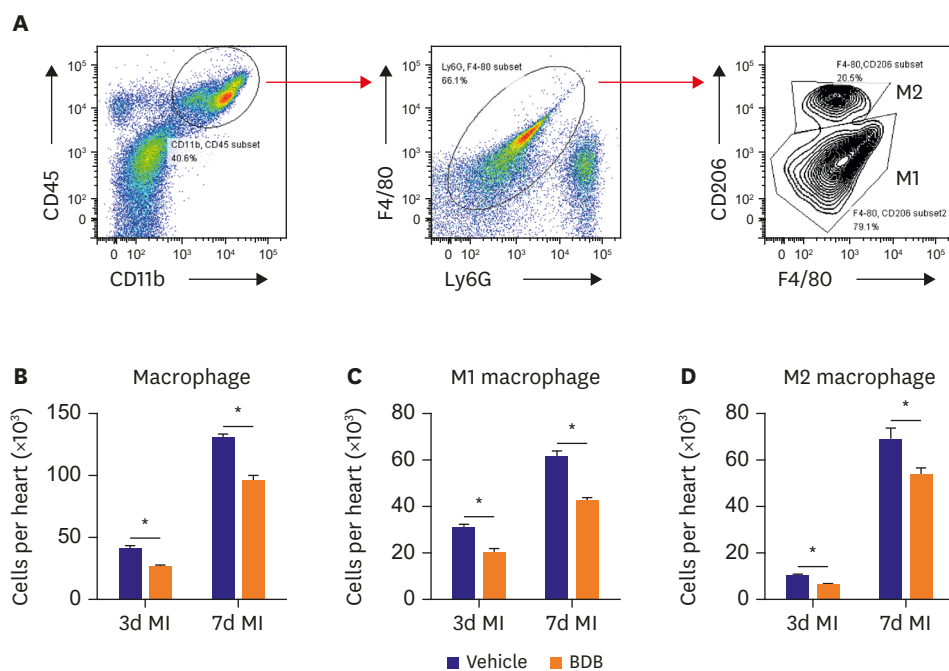


**Figure 4.** Treatment with BDB suppresses both M1 and M2 macrophage recruitment in hearts of mice after MI. (A) Gating strategy for CD11b<sup>+</sup>CD45<sup>+</sup>Ly6G<sup>-</sup>F4/80<sup>+</sup>CD206<sup>+</sup> and CD11b<sup>+</sup>CD45<sup>+</sup>Ly6G<sup>-</sup>F4/80<sup>+</sup>CD206<sup>-</sup> macrophages in hearts from BDB-treated mice after MI. (B-D) Effect of BDB treatment on the recruitment of (B) total macrophages, (C) M1, and (D) M2 macrophages in injured hearts from vehicle or BDB-treated mice on day 3 and 7 after MI. Data are expressed as mean±SEM (n=6-8). BDB = 3-Bromo-4,5-dihydroxybenzaldehyde; MI = myocardial infarction. \*The p<0.05 compared with vehicle group.

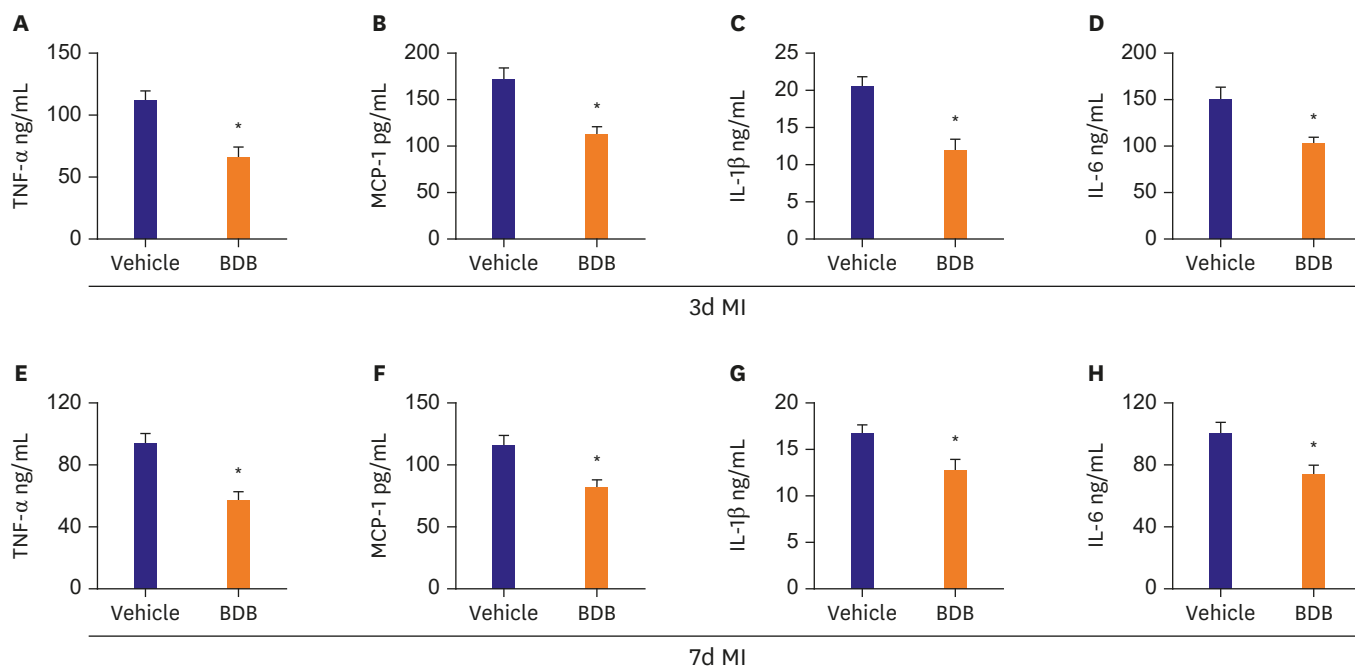


**Figure 5.** Administration of BDB reduced the levels of inflammatory cytokines in infarcted hearts. (A-D) Hearts from 3 days MI mice treated with vehicle and BDB (100 mg/kg) were evaluated for protein expressions by ELISA analysis; (A) TNF-α, (B) MCP-1, (C) IL-1β, and (D) IL-6. (E-H) Hearts from 7 days MI mice treated with vehicle and BDB (100 mg/kg) were evaluated for protein expressions by ELISA analysis: (E) TNF-α, (F) MCP-1, (G) IL-1β, and (H) IL-6. Data are expressed as mean±SEM (n=6-8). BDB = 3-Bromo-4,5-dihydroxybenzaldehyde; ELISA = enzyme-linked immunosorbent assay; IL = interleukin; MCP = monocyte chemoattractant protein; MI = myocardial infarction; TNF = tumor necrosis factor; SEM = standard error of measurement. \*The p<0.05 compared with vehicle group.



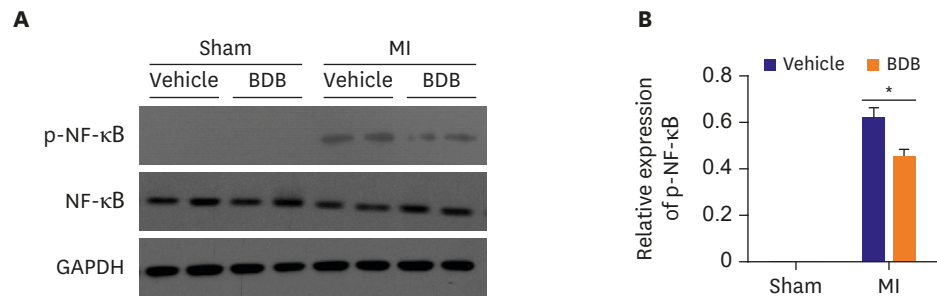


**Figure 6.** Effect of BDB on the NF-κB p65 phosphorylation in mice hearts of MI. (A) The protein level of phosphorylated NF-κB p65 in sham or infarcted hearts was analyzed by western blotting. (B) Quantification of phosphorylated NF-κB p65. Data are expressed as mean±SEM (n=4). BDB = 3-Bromo-4,5-dihydroxybenzaldehyde; GAPDH = glyceraldehyde 3-phosphate dehydrogenase; MI = myocardial infarction; NF = nuclear factor. \*The p<0.05 compared with vehicle group.

including IL-6 and TNF- $\alpha$ .<sup>16)</sup> The phosphorylation levels of NF-κB were significantly different between BDB treated group and vehicle treated group, BDB administration effectively down-regulated NF-κB phosphorylation in the hearts of MI while had no difference in the hearts of sham operation (**Figure 6A and B**). Taken together, the results showed that administration of BDB improved cardiac healing possibly via suppression of NF-κB phosphorylation.

## DISCUSSION

BDB is a therapeutic candidate by attenuating exacerbation of allergic inflammation such as atopic dermatitis and modulating the effects of oxidative stress.<sup>10)17)</sup> In the present study, we found that BDB conferred early cardioprotection after MI by inhibition macrophages recruitment and pro-inflammatory cytokines secretion, thereby improve the repair of injured heart after MI. Thus, our findings indicate that BDB may serve as a therapeutic agent for acute MI.

MI triggers an acute inflammatory response that is critical for cardiac repair but also participates in cardiac remodeling after ischemia and even heart failure. Pro-inflammatory macrophages are recruited into the infarcted myocardium in a sequential pattern.<sup>18)</sup> The macrophages subset accumulates in the injured heart on the first day after an MI, through MCP-1. Macrophages have highly inflammatory functions, as they secrete pro-inflammatory cytokines such as IL-1 $\beta$ , IL-6, and TNF- $\alpha$ .<sup>19)</sup> Thus, at day 1–7 after MI, the milieu in the heart is highly inflammatory, and macrophages plays very important role during this period. We found that, BDB inhibited the migrations of both macrophages into the infarcted hearts, subsequently facilitating cardiac repair by suppressing pro-inflammatory cytokine expression at early stages after MI.

BDB is a potent anti-inflammatory and a simple antioxidant compound mainly isolated from marine red algae, has been shown to inhibit inflammatory cell infiltration in the atopic dermatitis mouse model. NF-κB pathways is an important signaling that controls transcription, cytokines production and cell survival.<sup>20)</sup> NF-κB is found in almost all types of animal cell and is participated in many pathological and physiological processes such as stress, cytokines, free radicals, heavy metals, ultraviolet irradiation, cancer, and bacterial or viral antigens.<sup>21-23)</sup> NF-κB signaling activation leads to the transcription of early (TNF- $\alpha$ , IL-1 $\beta$ , and IL-6) inflammatory related genes.<sup>24)</sup> However, BDB has received relatively little attention

as an inflammatory-related agent in the MI model. Here we found that BDB can improve cardiac function recovery after MI in mice, attribute to reduce the infiltration of macrophage, including M1 and M2 macrophage, and the secretion of pro-inflammatory cytokines. The molecular mechanism is BDB strongly inhibited ischemia-induced phosphorylation of NF- $\kappa$ B.

In summary, we demonstrate first time that BDB confers cardioprotection after acute MI through reduced of macrophage recruitment into infarcted hearts, and decreased the secretion of pro-inflammation cytokines. These observations suggest that BDB may be used as an efficient therapeutic agent at the early stage of acute MI.

## REFERENCES

1. Aurora AB, Porrello ER, Tan W, et al. Macrophages are required for neonatal heart regeneration. *J Clin Invest* 2014;124:1382-92.  
[PUBMED](#) | [CROSSREF](#)
2. Maruotti N, Annese T, Cantatore FP, Ribatti D. Macrophages and angiogenesis in rheumatic diseases. *Vasc Cell* 2013;5:11.  
[PUBMED](#) | [CROSSREF](#)
3. Hofmann U, Frantz S. Role of lymphocytes in myocardial injury, healing, and remodeling after myocardial infarction. *Circ Res* 2015;116:354-67.  
[PUBMED](#) | [CROSSREF](#)
4. Fan X, Xu NJ, Shi JG. Bromophenols from the red alga *Rhodomela confervoides*. *J Nat Prod* 2003;66:455-8.  
[PUBMED](#) | [CROSSREF](#)
5. Li K, Li XM, Ji NY, Wang BG. Bromophenols from the marine red alga *Polysiphonia urceolata* with DPPH radical scavenging activity. *J Nat Prod* 2008;71:28-30.  
[PUBMED](#) | [CROSSREF](#)
6. Kim SY, Kim SR, Oh MJ, Jung SJ, Kang SY. In vitro antiviral activity of red alga, *Polysiphonia morrowii* extract and its bromophenols against fish pathogenic infectious hematopoietic necrosis virus and infectious pancreatic necrosis virus. *J Microbiol* 2011;49:102-6.  
[PUBMED](#) | [CROSSREF](#)
7. Piao MJ, Kang KA, Ryu YS, et al. The red algae compound 3-bromo-4,5-dihydroxybenzaldehyde protects human keratinocytes on oxidative stress-related molecules and pathways activated by UVB irradiation. *Mar Drugs* 2017;15:E268.  
[PUBMED](#) | [CROSSREF](#)
8. Hyun YJ, Piao MJ, Zhang R, Choi YH, Chae S, Hyun JW. Photo-protection by 3-bromo-4,5-dihydroxybenzaldehyde against ultraviolet B-induced oxidative stress in human keratinocytes. *Ecotoxicol Environ Saf* 2012;83:71-8.  
[PUBMED](#) | [CROSSREF](#)
9. Kim KC, Hyun YJ, Hewage SR, et al. 3-Bromo-4,5-dihydroxybenzaldehyde enhances the level of reduced glutathione via the Nrf2-mediated pathway in human keratinocytes. *Mar Drugs* 2017;15:E291.  
[PUBMED](#) | [CROSSREF](#)
10. Kang NJ, Han SC, Kang HJ, et al. Anti-inflammatory effect of 3-bromo-4,5-dihydroxybenzaldehyde, a component of *polysiphonia morrowii*, in vivo and in vitro. *Toxicol Res* 2017;33:325-32.  
[PUBMED](#) | [CROSSREF](#)
11. Kong D, Shen Y, Liu G, et al. PKA regulatory II $\alpha$  subunit is essential for PGD2-mediated resolution of inflammation. *J Exp Med* 2016;213:2209-26.  
[PUBMED](#) | [CROSSREF](#)
12. Vlasov IA, Volkov AM. Dependence of heart weight on body weight in patients with cardiovascular diseases. *Fiziol Cheloveka* 2004;30:62-8.  
[PUBMED](#)
13. Gaffney L, Warren P, Wrona EA, Fisher MB, Freytes DO. Macrophages' role in tissue disease and regeneration. *Results Probl Cell Differ* 2017;62:245-71.  
[PUBMED](#) | [CROSSREF](#)
14. Lavine KJ, Epelman S, Uchida K, et al. Distinct macrophage lineages contribute to disparate patterns of cardiac recovery and remodeling in the neonatal and adult heart. *Proc Natl Acad Sci U S A* 2014;111:16029-34.  
[PUBMED](#) | [CROSSREF](#)

15. Zhang JY, Yang Z, Fang K, Shi ZL, Ren DH, Sun J. Oleuropein prevents the development of experimental autoimmune myocarditis in rats. *Int Immunopharmacol* 2017;48:187-95.  
[PUBMED](#) | [CROSSREF](#)
16. Speranskii AI, Kostyuk SV, Kalashnikova EA, Veiko NN. Enrichment of extracellular DNA from the cultivation medium of human peripheral blood mononuclears with genomic CpG rich fragments results in increased cell production of IL-6 and TNF- $\alpha$  via activation of the NF- $\kappa$ B signaling pathway. *Biomed Khim* 2016;62:331-40.  
[PUBMED](#) | [CROSSREF](#)
17. Lee JC, Hou MF, Huang HW, et al. Marine algal natural products with anti-oxidative, anti-inflammatory, and anti-cancer properties. *Cancer Cell Int* 2013;13:55.  
[PUBMED](#) | [CROSSREF](#)
18. Nahrendorf M, Swirski FK, Aikawa E, et al. The healing myocardium sequentially mobilizes two monocyte subsets with divergent and complementary functions. *J Exp Med* 2007;204:3037-47.  
[PUBMED](#) | [CROSSREF](#)
19. Nahrendorf M, Swirski FK. Monocyte and macrophage heterogeneity in the heart. *Circ Res* 2013;112:1624-33.  
[PUBMED](#) | [CROSSREF](#)
20. Gilmore TD. Introduction to NF-kappaB: players, pathways, perspectives. *Oncogene* 2006;25:6680-4.  
[PUBMED](#) | [CROSSREF](#)
21. Perkins ND. Integrating cell-signalling pathways with NF-kappaB and IKK function. *Nat Rev Mol Cell Biol* 2007;8:49-62.  
[PUBMED](#) | [CROSSREF](#)
22. Capece D, Verzella D, Tessitore A, Alesse E, Capalbo C, Zazzeroni F. Cancer secretome and inflammation: the bright and the dark sides of NF- $\kappa$ B. *Semin Cell Dev Biol*. 2017 [Epub ahead of print].  
[PUBMED](#) | [CROSSREF](#)
23. Catrysse L, van Loo G. Inflammation and the metabolic syndrome: the tissue-specific functions of NF- $\kappa$ B. *Trends Cell Biol* 2017;27:417-29.  
[PUBMED](#) | [CROSSREF](#)
24. Han Y, Englert JA, Yang R, Delude RL, Fink MP. Ethyl pyruvate inhibits nuclear factor-kappaB-dependent signaling by directly targeting p65. *J Pharmacol Exp Ther* 2005;312:1097-105.  
[PUBMED](#) | [CROSSREF](#)